HUGONIOT SOUND VELOCITIES IN METALS WITH APPLICATIONS TO THE EARTH'S INNER CORE

Thomas S. DUFFY and Thomas J. AHRENS

Seismological Laboratory, California Institute of Technology, Pasadena, CA 91125, USA

Abstract. Hugoniot sound velocities in metals can be used to study the elastic properties of materials at high pressure. Both compressional and bulk sound velocities along the Hugoniot satisfy Birch's Law over the density range 2–27 g/cm^3. That is, velocities are linear in density with slopes proportional to atomic weight. This result provides empirical support for the validity of Birch's Law over the entire range of density distributions in the Earth's interior. Measured Hugoniot velocities are generally consistent with finite strain extrapolations of low pressure data. Differences between measured and extrapolated data can be attributed to thermal effects. Bulk sound velocities allow the volume dependence of the Gruneisen parameter, γ, to be constrained. In agreement with previous results for porous metals, the sound speed data for both solid and liquid metals are consistent with $q \equiv \partial ln\gamma / \partial ln V = 1$, where V is the volume. Shear velocity, V_S, can be constrained to ~4% along the Hugoniot in the best cases but more generally uncertainties exceed 10%. At compressions above $V_0/V \approx 1.43$, 3d- and 4d-series transition metals are characterized by negative dV_S/dP slopes ranging between –0.01 and –0.001 km/s/GPa. The low shear velocities result in values of Poisson's ratio above 0.4 for these materials, significantly greater than zero pressure values of 0.3–0.35. This suggests that the shear properties of the inner core are not anomalous but rather are characteristic of the type of behavior observed in 3d- and 4d-series metals at high pressure and temperature.

Introduction

The properties of the Earth's inner core remain poorly known because of the inaccessibility of the region to both seismological and laboratory studies. Recent seismological work, summarized by Masters and Shearer (1990), have improved our knowledge of the elasticity and other physical properties of the region. Shock wave studies have demonstrated that the density and elastic properties of iron are generally consistent with those of the core. Measurement of Hugoniot sound velocities (Brown and McQueen, 1986) has played an important role in this process. More generally, little is known about the variation of sound velocities under conditions appropriate to the Earth's deep interior. This is particularly unfortunate since the seismic velocity structure of the Earth is well known. Analysis of Hugoniot sound velocities therefore promises to yield clues to the elastic behavior of materials at high pressure and temperature.

The inner core, with a radius of about 1220 km, is believed to be a solid alloy composed dominantly of iron. The solidity of the inner core is inferred indirectly from free oscillation data which constrain the average shear velocity of the region to be 3.45 ± 0.1 km/s (Shearer and Masters, 1990). The rigidity of the inner core is much less than would be expected from low pressure data on iron and iron alloys. The average Poisson's ratio, σ, in the inner core from seismological observations is 0.44 (Dziewonski and Anderson, 1981). This value is anomalously high compared with most materials under normal conditions. σ increases as a function of both pressure and temperature but trends based on low-pressure ultrasonic data cannot explain the observed values. One possible explanation for this is that the inner core is partially molten, resulting in reduced rigidity (Loper and Fearn, 1983). Falzone and Stacey (1980) used second order elasticity theory to suggest that large values of σ are a natural consequence of the application of high pressure. This theory has not been tested using any high pressure elasticity data, however. A potentially serious limitation of the approach is that the calculated Voigt and Reuss bounds on the shear modulus diverge very rapidly at high pressure. Consequently, it is questionable whether the Voigt-Reuss-Hill average remains meaningful at large compressions for this theory.

Hugoniot sound velocities in iron have demonstrated the existence of two solid high-pressure phases in iron (Brown and McQueen, 1986). The ε-phase (hcp) is stable between 13 and 200 GPa along the Hugoniot. The second high pressure phase is stable between 200 and 243 GPa and it may be either the γ-(fcc) or α'-(bcc) phase (Anderson, 1986; Brown and McQueen, 1986; Ross *et al.*, 1990). Iron under inner core conditions is believed to be in the ε-phase on the basis of extrapolations of compressional velocity and Poisson's ratio (Brown and McQueen, 1986) as well as phase equilibria considerations (Anderson, 1986). The possibility that iron in the inner core is in the α' structure has also received consideration (Ross *et al.*, 1990).

In this study, the high-pressure elastic properties of metals will be investigated. The purpose will be to determine how accurately such properties can be constrained using available techniques. In addition, better understanding of the high pressure behavior of metals can be achieved by comparing metals with a wide range of properties. This information can then be applied to understanding the Earth's inner core.

Elastic properties at high pressure can be obtained from sound velocities measured under shock conditions. Shock wave techniques involve the dynamic generation of high pressures and temperatures in materials via high velocity plate impact (Ahrens, 1987). The measurement of sound

High-Pressure Research: Application to Earth and Planetary Sciences, edited by Y. Syono and M. H. Manghnani, pp. 353 – 361.

velocities behind the shock front relies on two primary techniques known as the VISAR and the optical analyzer methods (Barker and Hollenbach, 1972; McQueen *et al.*, 1982). In both techniques, a one-dimensional rarefaction front is developed when the shock wave reflects from the free surface at the rear of the thin impacting plate. This wave travels back through the sample and is detected optically. The velocity of the leading edge of this front represents the high pressure sound velocity in the sample. This velocity will either be the compressional velocity, V_P, for a solid sample or the bulk velocity, V_B, for a liquid sample or one that has been shock-melted. Sound velocities are typically determined to 1–3% precision using these techniques.

The usefulness of Hugoniot sound velocity measurements lies in the fact that they provide information about the elastic properties of materials at simultaneous high pressure and temperature. This information cannot currently be obtained in any other way. Other techniques, such as ultrasonic interferometry, although of intrinsically much greater precision, are limited to relatively low pressures (a few GPa). Sound velocity measurements yield information about the Gruneisen parameter, γ, as discussed below. While compression data provide information about the bulk modulus and its pressure dependence at high pressure, sound velocity data are the only means to obtain information about the rigidity at high pressure.

Hugoniot Sound Velocities

Compressional Velocities

Figure 1 presents a summary of compressional sound velocity data for shock-loaded metals. While the figure is not meant to be an exhaustive compilation, it is representative in the sense that a variety of types of metals are included. The figure illustrates that Hugoniot compressional velocities satisfy Birch's law. A general velocity-density relationship derivable from lattice dynamics is (Anderson, 1967; Shankland and Chung, 1974):

$$V_P = A\rho^{\lambda} \tag{1}$$

where ρ is the density and A and λ are constants which depend on atomic weight. The linear approximation to this relationship is known as Birch's law:

$$V_P = a + b\rho \tag{2}$$

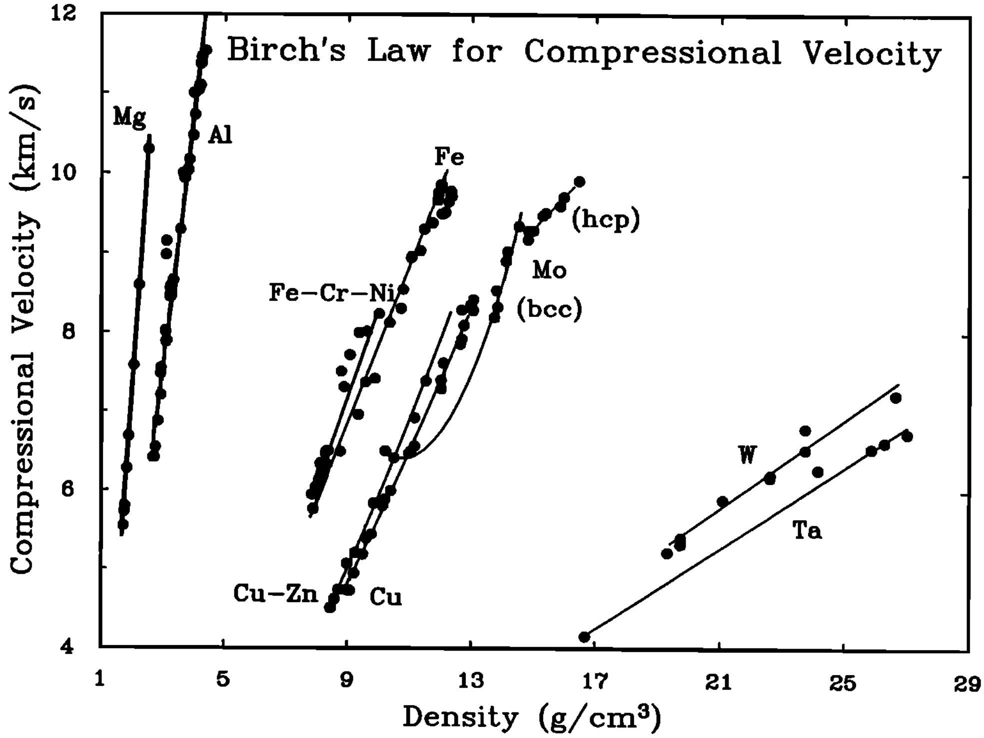

Figure 1. Hugoniot compressional velocity for metals plotted against density demonstrating the validity of Birch's law along the Hugoniot. Solid lines are least squares fits to the data. References for the data are Al (Neal, 1976; Asay and Chhabildas, 1981; McQueen *et al.*, 1984; Asay *et al.*, 1986); Mg (Wang, 1988); Fe-Cr-Ni (Duffy and Ahrens, 1990); Fe (Barker and Hollenbach, 1974; Brown and McQueen, 1986; Wang, 1988); Cu-Zn (Wang *et al.*, 1987; Wang, 1988); Cu (Chhabildas and Asay, 1982; Wang, 1988; Hu *et al.*, 1989); Mo (Hixson *et al.*, 1989); Ta (Brown and Shaner, 1984; Asay *et al.*, 1986); W (Chhabildas *et al.*, 1988).

where a and b are constants. At low pressures, the validity of Birch's law for compressional velocity has been demonstrated repeatedly (e.g. Birch, 1961a; Shankland and Chung, 1974). Figure 1 demonstrates its applicability to high pressure measurements of compressional velocity along the Hugoniot as well. The slopes in Eq. (2) are up to a factor of 2.5 lower under Hugoniot conditions than observed ultrasonically along both the $P = 0$ isobar and the 300 K isotherm for these materials. The only clear exception to Birch's Law is the data for bcc molybdenum which do not linearly extrapolate back to the zero pressure compressional velocity. The anomalous behavior of this material has been attributed to a pressure induced s→d electronic transfer (Hixson *et al.*, 1989; Godwal and Jeanloz, 1990).

Another feature of Fig. 1 in common with typical Birch plots is that the slopes of the $V_P - \rho$ relations are decreasing functions of atomic weight. Birch (1961b) demonstrated that the hydrodynamic velocity obtained from differentiating the Hugoniot curve satisfies Birch's Law. Shaner *et al.* (1988) demonstrated the validity of Birch's law for the isentropic bulk sound velocity, V_B, measured in shock-melted metals. This result was extended to a suite of liquid alkali halides by Boness and Brown (1990). In general, Birch's law has better theoretical justification for bulk velocities rather than compressional or shear velocities because of the influence of non-central forces in determining the rigidity (Shankland and Chung, 1974). Nevertheless, Fig. 1 shows that Birch's law remains valid along the Hugoniot for V_P to large compression. For the materials studied here, there is little difference between the functional forms of Eqs. (1) and (2). There is presently less data with which to test Birch's law for minerals but available data for Al_2O_3 and the high pressure phases of SiO_2 and Mg_2SiO_4 give some indication that Birch's law holds for V_P for minerals on the Hugoniot as well (Barker and Hollenbach, 1970; Chhabildas and Miller, 1985; Brown *et al.*, 1987). Additionally, limited bulk sound velocity data for solid metals (aluminum and tungsten) also suggest the applicability of Birch's Law to V_B in solid metals.

The applicability of Birch's law under Hugoniot conditions suggests that it could be a useful method to extend measured data to higher and lower pressure Hugoniot states. For example, comparison of Fe and Fe-Cr-Ni compressional velocities (Fig. 1) indicates that the iron alloy has faster velocities than pure iron. Extrapolation of these results to inner core conditions using Birch's law suggest that compressional velocities in the inner core can be satisfied by the incorporation of 5–10% transition metal impurity (Duffy and Ahrens, 1990).

The above discussion raises a significant issue. With the exception of shock data, most laboratory measurements of sound velocity are limited to pressures of only a few GPa at present. The velocities are often extrapolated to high pressure using an equation of state such as the third-order Eulerian finite strain equations (Birch, 1938; Sammis *et al.*, 1970) for comparison with seismic data. While there is a large amount of data supporting the use of this equation for compression data (e.g. Jeanloz, 1989b), its use for sound velocities, particularly the shear velocity, has weaker empirical support (Birch, 1978). One application of Hugoniot sound velocities then is to compare them with extrapolations of low pressure data, bearing in mind that differences in thermal states may be quite large.

Figure 2 shows Hugoniot sound velocities for several metals compared with third-order finite-strain extrapolations based on low-pressure ultrasonic data. The most striking feature of the figure is that the difference between the extrapolated and measured data is small (less than 10%), despite the fact that the Hugoniot states may be hotter by many thousands of K. The Hugoniot data lie systematically below predicted isentropic curves, which is consistent with the interpretation that the differences between the two curves are related to thermal effects. Based on zero pressure temperature coefficients of velocity, one would predict that Hugoniot velocities should be up to a third less than finite strain predictions at high pressure. This result is illustrated for aluminum in Fig. 2. Duffy and Ahrens (1992) have used this data to determine that the magnitude of the temperature coefficient of velocity decreases strongly as a function of pressure. The comparison of Fig. 2 neglects both temperature effects and higher order pressure effects on the velocities.

Shear Velocities

Jeanloz (1989a) has pointed out that Hugoniot compressional velocities and equation of state (EOS) data can be combined to constrain the shear velocity along the Hugoniot. In this section, we investigate the precision with which the shear velocities can be constrained using this procedure and apply it to a series of metals. Results will then be compared with seismological data for the inner core.

Shear velocities can be directly measured under Hugoniot conditions by, for example, pressure-shear loading (Chhabildas and Swegle, 1980) but at present these techniques are limited to low pressures and are of low precision. Compressional velocities measured along the Hugoniot contain information about the shear modulus, however. The Hugoniot density is constrained from conservation of mass across the shock front. For solids, the bulk velocity can, in some cases, be measured along with the compressional velocity in a VISAR or optical analyzer experiment (e.g. McQueen *et al.*, 1984; Chhabildas *et al.*, 1988). More generally, however, only the fastest velocity V_P (solid) or V_B (liquid) can be readily determined. EOS data also yield information about the bulk modulus at high pressure.

In the absence of phase changes, shock data for most materials can be described by a linear shock wave equation of state:

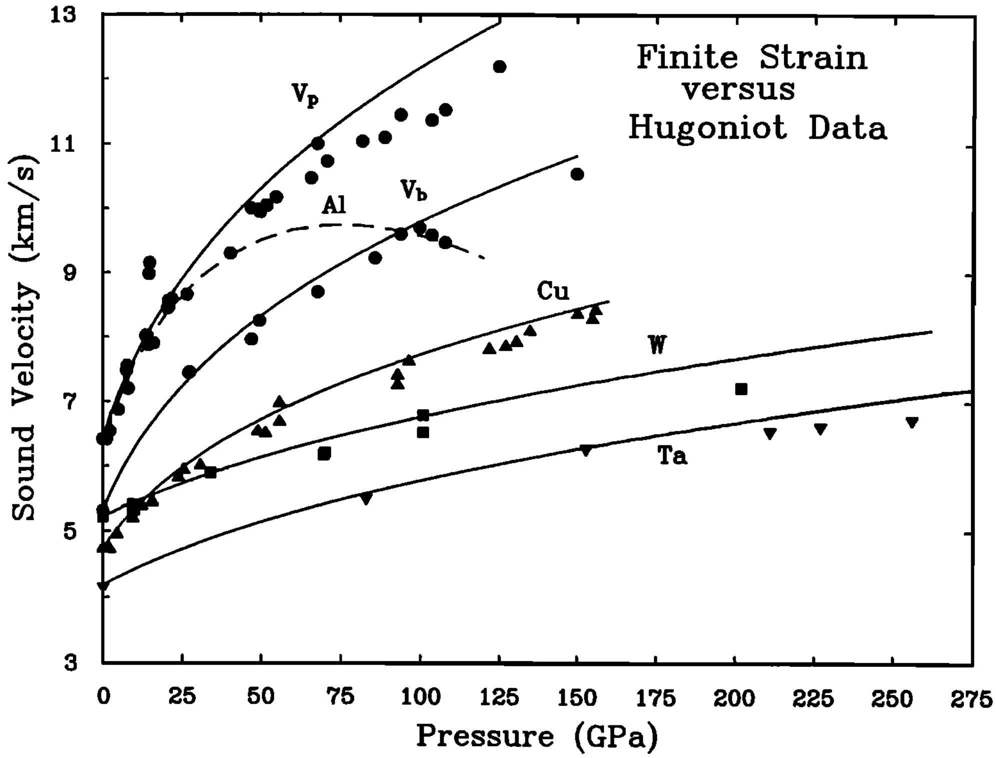

Figure 2. Comparison of Hugoniot sound velocity data with finite strain extrapolations. The solid curves are extrapolations based on third order Eulerian finite strain theory using elastic coefficients determined from low pressure ultrasonic experiments. Hugo niot states become increasingly hotter than isentropic extrapolations at high pressure. The Hugoniot data (solid symbols) are a subset of those in Fig. 1 and include bulk sound velocities determined for solid aluminum. The dashed curve represents expected compressional velocities in aluminum along the Hugoniot if the temperature coefficient of velocity remains constant at its zero pressure value. References for the data are listed in Fig. 1. The parameters for the finite strain extrapolations are compiled in Simmons and Wang (1971).

$$U_S = c_0 + su_p \tag{3}$$

where U_S is the shock wave velocity, u_p is the particle velocity behind the shock front, and c_0 and s are material constants. Pressure-volume-energy states achieved upon shock compression are obtained from expressions for conservation of mass, momentum, and energy across the shock front known collectively as the Rankine-Hugoniot equations. The bulk modulus at high pressure can be determined from the EOS using the Mie-Gruneisen equation. The Gruneisen parameter can be defined as:

$$\gamma = V\left(\frac{\partial P}{\partial E}\right)_V = \frac{\alpha V K_S}{C_P} \tag{4}$$

where V is volume, P is pressure, E is specific energy, α is the coefficient of thermal expansion, K_S is the adiabatic bulk modulus, and C_P is the specific heat at constant pressure. The Gruneisen parameter is useful in describing the relationship between the Hugoniot and other thermodynamic paths as well as in describing, for example, the melting curve and the adiabatic gradient. The Gruneisen parameter also relates the Hugoniot to the release isentrope from the high-pressure state, allowing the bulk sound speed to be determined from:

$$V_B = V\left(\frac{-\partial P}{\partial V}\right)_S^{1/2} \tag{5}$$

In terms of Hugoniot parameters, the bulk sound velocity can be written (McQueen *et al.*, 1967):

$$V_B^2 = V^2\left[\left(\frac{\partial P}{\partial V}\right)_H \left[(V_o - V)\frac{\gamma}{2V} - 1\right] + \frac{P\gamma}{2V}\right] \tag{6}$$

where H represents Hugoniot conditions and the subscript o represents ambient conditions.

Thus, knowledge of both the shock wave equation of state and the Gruneisen parameter constrains the bulk sound velocity. Conversely, measurement of the bulk sound veloc-

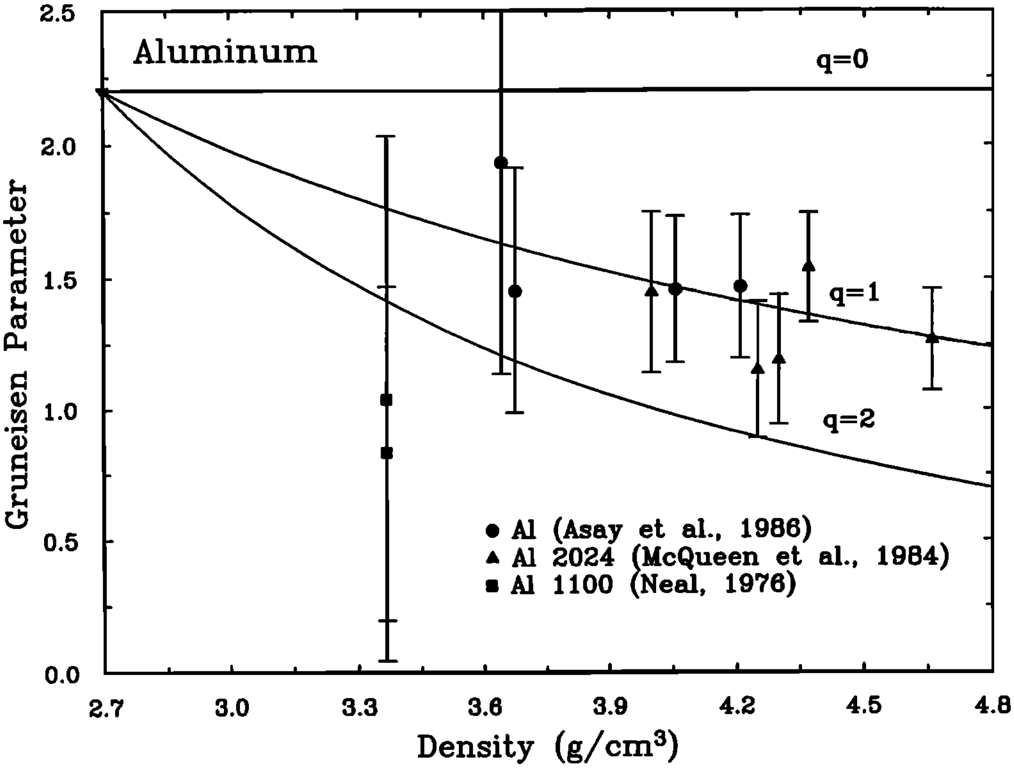

Figure 3. Gruneisen parameter as a function of density for aluminum. Data points are derived from Hugoniot bulk sound velocity measurements on solid aluminum except for the highest pressure datum which is liquid. The zero pressure thermodynamic Gruneisen parameter is shown by the inverted triangle. Solid curves represent a range of possible volume dependence for γ following Eq. (7) with q values of 0, 1 and 2.

ity and the EOS yields the Gruneisen parameter. It is often assumed that γ depends only on volume:

$$\gamma = \gamma_o \left(\frac{V}{V_o} \right)^q \tag{7}$$

In many cases, the parameter $q = d\ln\gamma / d\ln V$ is assumed to be 1.

In order to test assumptions about the parameter q, bulk sound velocity data were used to constrain γ at high pressure. An example of these results are shown in Fig. 3 where Gruneisen parameter values are shown for aluminum. The precision of the measured γ values increases strongly with compression because the slopes of the Hugoniot and the adiabat diverge with increasing pressure. Also shown in the figure are curves representing several different values for the parameter q in Eq. (7). All the aluminum data are consistent with $q = 1$ (that is, $\rho\gamma =$ constant). Weighted least squares fits combining Hugoniot results with the zero pressure thermodynamic Gruneisen parameter were used to determine q values for several metals. The results of these fits are listed in Table 1. All the materials studied are consistent with q values near 1 within their respective uncertainties. This conclusion holds whether the material is solid or liquid and appears to hold across the solid-melt boundary in aluminum. The level of uncertainty on q depends strongly on knowledge of the STP Gruneisen parameter. The effect of phase changes on the Gruneisen parameter represent a significant area of uncertainty. For iron, the estimated zero pressure Gruneisen parameter (Table 1) is based on the thermodynamic and EOS properties of ε-iron (Manghnani *et al.*, 1987; Mao *et al.*, 1990) and an assumed specific heat of 3R. If only the high pressure γ values are used to constrain q, a least squares fit yields $q = 0.1 \pm 1.2$ and $\gamma_0 = 1.7$. This illustrates that there remains considerable uncertainty in the volume dependence of γ for iron.

The results of Table 1 in conjunction with Eqs. (6) and (7) constrain V_B on the Hugoniot. In cases where liquid data was used to obtain q, there is the additional assumption that the bulk sound velocity (and the Gruneisen parameter) varies smoothly across the melting boundary. By combining these values with measured compressional velocities, the shear velocity can be determined from:

TABLE 1. Volume Dependence of Gruneisen Parameter

Material	State	# of data	γ_0	q	Reference
Al	solid	11	2.2	1.1 ± 0.2	McQueen *et al.*, 1984 Asay *et al.*, 1986 Neal, 1976
Ta	liquid	6	1.7	0.9 ± 0.2	Brown and Shaner, 1984
W	solid	6	1.7	0.5 ± 0.5	Chhabildas *et al.*, 1988
Cu-Zn	liquid	4	2.0	1.3 ± 0.2	Wang *et al.*, 1987
ε-Fe	liquid	4	2.3	0.8 ± 0.5	Brown and McQueen, 1986
Mo	liquid	3	1.7	1.1 ± 0.2	Hixson *et al.*, 1989
Cu	liquid	1	2.0	0.9 ± 0.5	Hu *et al.*, 1989
Fe-Cr-Ni	–	–	1.4	1.0**	Duffy and Ahrens, 1990
Mg	–	–	1.4	1.0**	Wang, 1988

*Highest pressure datum in liquid state.
**Assumed.

$$V_S^2 = \frac{3}{4}\left(V_P^2 - V_B^2\right) \tag{8}$$

Results for the metals are shown in Fig. 4. Typically, Hugoniot and Gruneisen parameter data constrain the bulk sound velocity to ±3% and the shear velocity is uncertain by ±10% or more. Aluminum represents the best possible case in that both V_P and V_B are measured to ~1% which in combination yield a shear velocity constrained to ~4%.

At small compressions, shear velocity data satisfy Birch's law: velocities are linear in density with slopes proportional to atomic weight. However, for the 3d- and 4d-series transi-

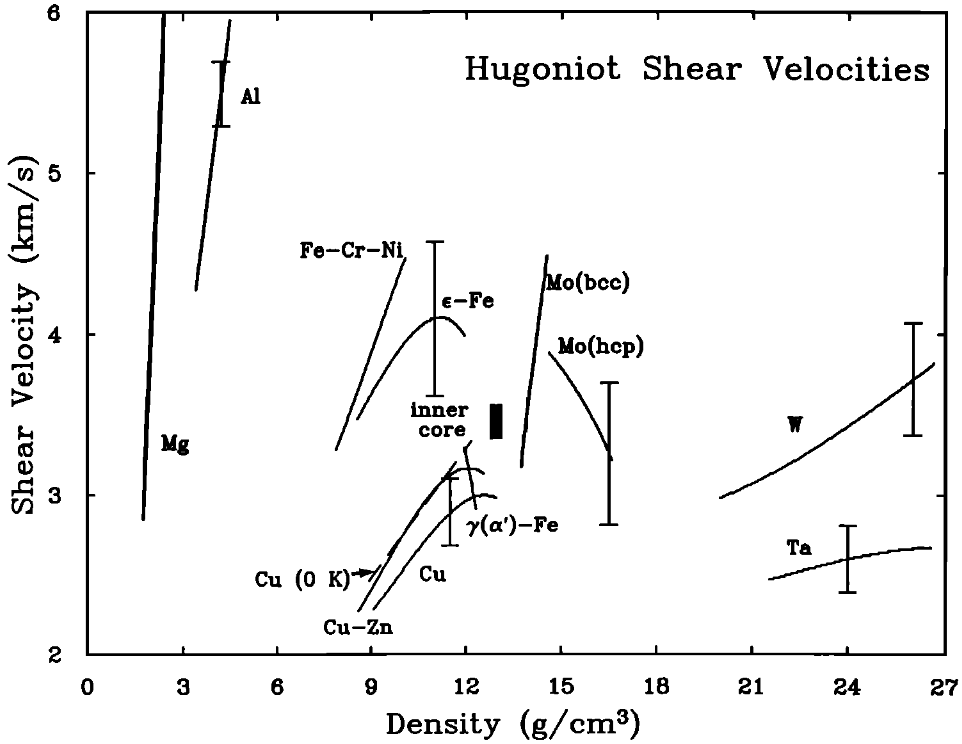

Figure 4. Shear velocities along the Hugoniot for metals. Data are plotted over a range spanning the compressional sound velocity measurements for each material. Representative error bars are shown at selected densities for some materials. The range of possible inner cores values (Masters and Shearer, 1990) is indicated by the box. The dashed curve represents a pseudopotential calculation (Straub *et al.*, 1988) for copper. The high pressure solid phase of iron may be either in the γ(fcc) or α'(bcc) structures. Sources for data are listed in the Fig. 1 caption.

tion metals and alloys (Cu, Cu-Zn, Fe, Fe-Cr-Ni, Mo), the shear velocity slopes flatten and become negative at compressions above $V_0/V = 1.43 \pm 0.05$. For Cu, Mo, Fe, and Cu-Zn, the shear velocity slopes above this compression lie between –0.01 and –0.001 km/s/GPa. The high-pressure phases of both iron (δ or α') and molybdenum (hcp) have negative shear velocity slopes. Given the large uncertainties, the decrease in shear velocity at large compression cannot be unequivocally demonstrated. The tendency for this type of behavior is restricted to certain metals, however. Neither the lighter metals nor the heavier transition metals exhibit such decreases even near their melting points (Al, Ta).

Calculated Hugoniot shear velocities lie below finite strain extrapolations but such comparisons are not very meaningful given the large uncertainties and thermal differences between the curves. Elastic moduli in copper have been calculated as a function of pressure (at 0 K) using a pseudopotential model (Straub *et al.*, 1988) (Fig. 4). The slopes of the theoretical and calculated shear velocities for this material are similar except at large compression. Shear velocities in the high pressure phases of iron, and in the 3d- and 4d-series transition metals generally, are broadly consistent with inner core shear velocities. Shear velocities in the high pressure iron phases are particularly uncertain at large compressions because of the uncertainty in the behavior of the Gruneisen parameter.

Poisson's Ratio

Compressional and shear velocities can be combined to yield Poisson's ratio, σ, using the following expression:

$$\sigma = \frac{1}{2}\frac{(V_P / V_S)^2 - 2}{(V_P / V_S)^2 - 1} \qquad (9)$$

Poisson's ratio values for metals along the Hugoniot are shown in Fig. 5. Uncertainties are typically ±5–10%. Because of their anomalous shear properties, 3d- and 4d-series transition elements are characterized by large increases in σ with compression. This is not evident in either the 5d transition elements or the lighter metals. Mg and bcc Mo are anomalous in that σ decreases with compression for these materials. The trends established by the 3d and 4d transition metals in general and the two high pressure phases of iron in particular are comparable to the seismologically determined Poisson's ratio for the inner core. It appears that the large

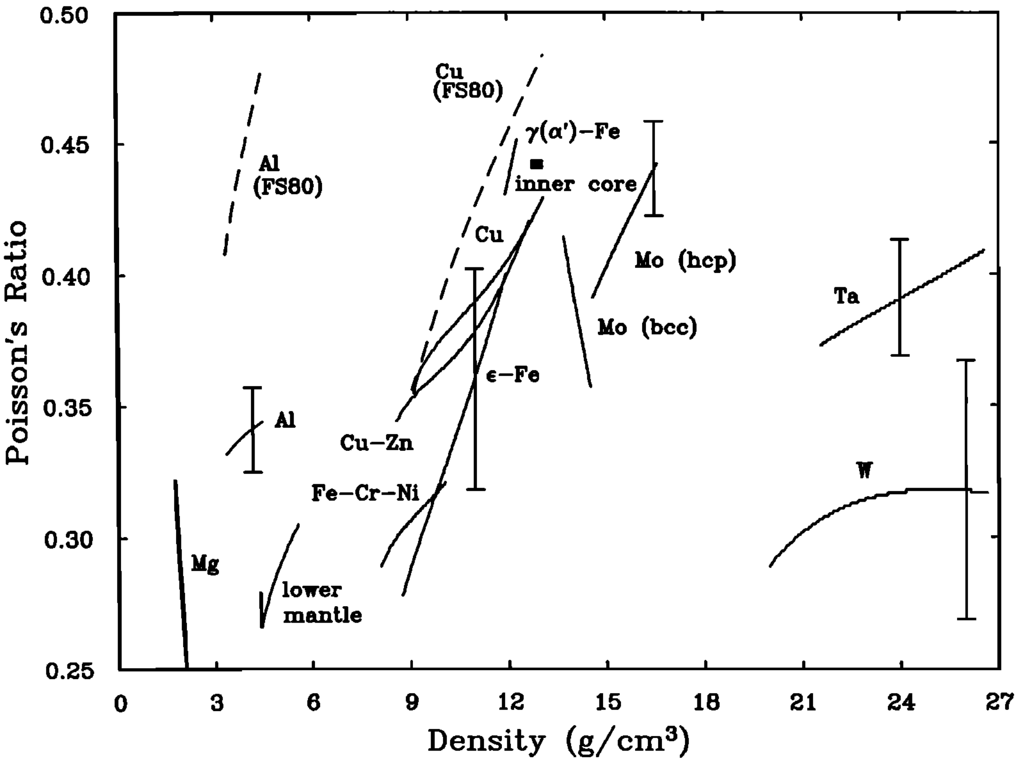

Figure 5. Poisson's ratio along the Hugoniot for metals. The values were derived from compressional velocities of Fig. 1 and shear velocities of Fig. 4. Representative error bars are shown at selected densities for some materials. The range of possible inner cores values from Earth model PREM (Dziewonski and Anderson, 1981) is indicated by the box. Mantle values are also from PREM. The dashed curves represent the predictions of Falzone and Stacey (1980) for aluminum and copper.

value of σ observed in the inner core is not anomalous but may be representative of typical behavior of 3d and 4d transition metals and alloys. Also shown in the figure are results for Al and Cu using the theory of Falzone and Stacey (1980) which significantly overestimates the observed values of Poisson's ratio. While quantitative agreement is not obtained, qualitative agreement is achieved in the sense that the Hugoniot data demonstrate that large values of Poisson's ratio do occur at high pressures, at least for certain type of materials. This further implies that partial melting is not required to explain the shear properties of the Earth's inner core (Loper and Fearn, 1983).

Summary

Analysis of Hugoniot sound velocities in metals leads to a number of geophysically significant results. Hugoniot compressional and bulk velocities satisfy Birch's law for densities between 2 and 27 g/cm^3. That is, velocity is linear with density with a slope proportional to atomic weight. This fundamental description of material behavior offers a means to extrapolate sound velocities to higher and lower pressure Hugoniot states. Furthermore, it provides strong empirical support for the applicability of Birch's Law over the entire pressure and temperature regime of the Earth. Compressional and bulk sound velocities are also broadly consistent with the predictions of third-order Eulerian finite strain theory. Deviations between data and extrapolations increase with pressure and these deviations can be attributed to thermal effects.

Constraints on the volume dependence of the Gruneisen parameter can be obtained from the combination of Hugoniot EOS and sound speed data. Results for metals, both solids and liquids, are uniformly consistent with the result $q = \partial ln\gamma/\partial ln V = 1$ (that is, γ/V = constant). In the best cases, bulk sound velocity data constrain q to about ±20%. However, a major unresolved problem is how γ varies across solid-solid and solid-liquid phase boundaries. For iron, constraints on q are particularly weak because of uncertainty regarding the appropriate zero-pressure Gruneisen parameter. The high-pressure data alone are insufficient to distinguish between $q = 0$ and $q = 1$. Nevertheless, the data set considered as a whole supports the use of γ/V = constant for metals. This is consistent with the results obtained from shock compression of porous materials (McQueen *et al.*, 1970).

Hugoniot sound velocities provide constraints on shear properties. In the best circumstances (e.g. aluminum) where precise measurements of V_P and V_B in the solid state are available, the shear velocity is constrained to ~4%. More generally, where EOS data are used to determine V_B, the uncertainty in V_S exceeds 10%. Detailed comparisons with seismological data are probably not warranted for such data. Poisson's ratio can be constrained to within 5–10% by existing data.

The metals studied here can be divided into two classes on the basis of high-pressure shear properties. At V_0/V above 1.43, the 3d- and 4d-series transition metals are characterized by $\partial V_S/\partial P < 0$, with slopes ranging from –0.01 to –0.001 km/s/GPa. This results in values of Poisson's ratio greater than 0.4 at high pressure. Neither the light nor the heavy metals (Al, Ta, W) exhibit such behavior. The shear properties of the inner core appear to be characteristic of the type of behavior exhibited by the 3d and 4d metals under high compression. Therefore, the seismic shear properties of the inner core may not require the presence of partial melt and may be related to $\partial V_S/\partial P < 0$ at high pressure and temperature.

Acknowledgments. We appreciate the comments of Don L. Anderson, J. M. Brown, and an anonymous reviewer. This research was supported by NSF grant EAR-8816669. Contribution 5006, Division of Geological and Planetary Sciences, California Institute of Technology.

REFERENCES

Ahrens, T. J., Shock wave techniques for geophysics and planetary physics, in *Methods of Experimental Physics*, vol. 24, edited by C. G. Sammis and T. L. Henyey, pp. 185–235, Academic, New York, 1987.

Anderson, D. L., A seismic equation of state, *Geophys J. R. Astron. Soc.*, *13*, 9–30, 1967.

Anderson, O. L., Properties of iron at the Earth's core conditions, *Geophys. J. R. Astron. Soc.*, *84*, 561–579, 1986.

Asay, J. R. and L. C. Chhabildas, Determination of the shear strength of shock compressed 6061-T6 aluminum, in *Shock Waves and High Strain-Rate Phenomena in Metals*, edited by M. A. Meyers and L. E. Murr, pp. 417–431, Plenum, New York, 1981.

Asay, J. R., L. C. Chhabildas, G. I. Kerley, and T. G. Trucano, High pressure strength of shocked aluminum, in *Shock Waves in Condensed Matter—1985*, edited by Y. M. Gupta, pp. 145–149, Plenum, New York, 1986.

Barker, L. M. and R. E. Hollenbach, Shock-wave studies of PMMA, fused silica, and sapphire, *J. Appl. Phys.*, *41*, 4208–4226, 1970.

Barker, L. M. and R. E. Hollenbach, Laser interferometer for measuring high velocities of any reflecting surface, *J. Appl Phys.*, *43*, 4669–4675, 1972.

Barker, L. M. and R. E. Hollenbach, Shock wave study of the $\alpha \Leftrightarrow \varepsilon$ phase transition in iron, *J. Appl. Phys.*, *45*, 4872–4887, 1974.

Birch, F., The effect of pressure upon the elastic properties of isotropic solids according to Murnaghan's theory of finite strain, *J. Appl. Phys.*, *9*, 279–288, 1938.

Birch, F., The velocity of compressional waves in rocks to 10 kilobars 2, *J. Geophys. Res.*, *66*, 2199–2224, 1961a.

Birch, F., Composition of the Earth's mantle, *Geophys. J. R. Astron. Soc.*, *4*, 295–311, 1961b.

Birch, F., Finite strain isotherm and velocities for singe-crystal and polycrystalline NaCl at high pressures and 300 K, *J. Geophys. Res.*, *83*, 1257–1268, 1978.

Boness, D. A. and J. M. Brown, Time-resolved optical spectroscopy of shock-compressed fluid alkali halides, in *Shock Waves in Condensed Matter—1989*, edited by S. C. Schmidt, J. N. Johnson, and L. W. Davison, pp. 863–866, North-Holland, New York, 1990.

Brown, J. M., M. D. Furnish, and R. G. McQueen, Thermodynamics for $(Mg, Fe)_2SiO_4$ from the Hugoniot, in *High Pressure Research in*

Mineral Physics, edited by M. H. Manghnani and Y. Syono, pp. 373–384, AGU, Washington, 1987.

Brown J. M. and R. G. McQueen, Phase transitions, Gruneisen parameter, and elasticity for shocked iron between 77 GPa and 400 GPa, *J. Geophys. Res.*, *91*, 7485–7494, 1986.

Brown, J. M. and J. W. Shaner, Rarefaction velocities in shocked tantalum and the high pressure melting point, in *Shock Waves in Condensed Matter—1983*, edited by J. R. Asay, R. A. Graham, and G. K. Straub, pp. 91–94, Elsevier, New York, 1984.

Chhabildas, L. C. and J. R. Asay, Time-resolved wave profile measurements in copper to megabar pressures in High Pressure in *Research and Industry*, 8th AIRAPT Conf., edited by C. M. Backman, T. Johannisson, and L. Tegman, pp. 183–189, 1982.

Chhabildas, L. C., J. R. Asay, and L. M. Barker, Shear strength of tungsten under shock- and quasi-isentropic loading to 250 GPa, Sandia Natl. Lab., *Rep. SAND88-0306*, 1988.

Chhabildas, L. C. and J. M. Miller, Release-adiabat measurements in crystalline quartz, Sandia Natl. Lab., *Rep. SAND85–1092*, 1985.

Chhabildas, L. C. and J. W. Swegle, Dynamic pressure-shear loading of materials using anisotropic crystals, *J. Appl. Phys.*, *51*, 4799–4807, 1980.

Duffy, T. S. and T. J. Ahrens, Sound velocities and wave profiles in an iron alloy shocked to 74 GPa, *EOS, Trans. AGU*, *71*, 1639, 1990.

Duffy, T. S. and T. J. Ahrens, Sound velocities at high pressure and temperature and their geophysical implications, in press, *J. Geophys. Res.*, 1992.

Dziewonski, A. D. and D. L. Anderson, Preliminary reference Earth model, *Phys. Earth Planet. Int.*, *25*, 297–356, 1981.

Falzone, A. J. and F. D. Stacey, Second-order elasticity theory: explanation for the high Poisson's ratio of the inner core, *Phys. Earth Planet. Int.*, *21*, 371–377, 1980.

Godwal, B. K. and R. Jeanloz, Pressure-induced s→d transfer and the equation of state of molybdenum, *Phys. Rev. B*, *41*, 7440–7445, 1990.

Hixson, R. S., D. A. Boness, J. W. Shaner, and J. A. Moriarty, Acoustic velocities and phase transitions in molybdenum under shock compression, *Phys. Rev. Lett.*, *62*, 637–640, 1989.

Hu, J., F. Jing, and J. Cheng, Sound velocities at high pressures and shock-melting of copper, *Chin. J. High Pressure Phys.*, *3*, 187–197, 1989.

Jeanloz, R., High pressure chemistry of the Earth's mantle and core, in *Mantle Convection: Plate Tectonics and Global Dynamics*, edited by W. R. Peltier, pp. 203–260, Gordon and Breach, 1989a.

Jeanloz, R., Shock-wave equation of state and finite strain theory, *J. Geophys. Res.*, *94*, 5873-5886, 1989b.

Loper, D. E. and D. R. Fearn, A seismic model of a partially molten inner core, *J. Geophys. Res.*, *88*, 1235–1242, 1983.

Manghnani, M. H., L. C. Ming, and N. Nakagiri, Investigation of the α-Fe-ε-Fe phase transition by synchrotron radiation, in *High-Pressure Research in Mineral Physics*, edited by M. H. Manghnani and Y. Syono, pp. 155–163, AGU, Washington, 1987.

Mao, H. K., Y. Wu, L. C. Chen, and J. F. Shu, Static compression of iron to 300 GPa and $Fe_{0.8}Ni_{0.2}$ alloy to 260 GPa: Implications for composition of the core, *J. Geophys. Res.*, *95*, 21,737–21,742, 1990.

Masters, T. G. and P. M. Shearer, Summary of seismological constraints on the structure of the Earth's core, *J. Geophys. Res.*, *95*, 21,691–21,695, 1990.

McQueen, R. G., J. N. Fritz, and C. E. Morris, The velocity of sound behind strong shock waves in 2024 Al, in *Shock Waves in Condensed Matter—1983*, edited by J. R. Asay, R. A. Graham, and G. K. Straub, pp. 95–98, Elsevier, New York, 1984.

McQueen, R. G., J. W. Hopson, and J. N. Fritz, Optical technique for determining rarefaction wave velocities at very high pressures, *Rev. Sci. Instr.*, *53*, 245–250, 1982.

McQueen, R. G., S. P. Marsh, and J. N. Fritz, Hugoniot equation of state of twelve rocks, *J. Geophys. Res.*, *72*, 4999-5035, 1967.

McQueen, R. G., S. P. Marsh, J. W. Taylor, J. N. Fritz, and W. J. Carter, The equation of state of solids from shock wave studies, in *High-Velocity Impact Phenomena*, edited by R. Kinslow, pp. 294–419, Academic Press, New York, 1970.

Neal, T., Dynamic determination of the Gruneisen coefficient in aluminum and aluminum alloys for densities up to 6 Mg/m^3, *Phys. Rev. B*, *14*, 5172-5181, 1976.

Ross, M., D. A. Young, and R. Grover, Theory of the iron phase diagram at Earth core conditions, *J. Geophys. Res.*, *95*, 21,713–21,716, 1990.

Shankland, T. J. and D. H. Chung, General relationships among sound speeds II. Theory and discussion, *Phys. Earth Planet. Int.*, *8*, 121–129, 1974.

Sammis, C., D. Anderson, and T. Jordan, Application of isotropic finite strain theory to ultrasonic and seismological data, *J. Geophys. Res.*, *75*, 4478–4480, 1970.

Shaner, J. W., R. S. Hixson, M. A. Winkler, D. A. Boness, and J. M. Brown, Birch's law for fluid metals, in *Shock Waves in Condensed Matter—1987*, edited by S. C. Schmidt and N. C. Holmes, pp. 135–138, North-Holland, New York, 1988.

Shearer, P. M. and G. Masters, The density and shear velocity contrast at the inner core boundary, *Geophys. J. Int.*, *102*, 491–498, 1990.

Simmons, G. and H. Wang, *Single Crystal Elastic Constants and Calculated Aggregate Properties: A Handbook*, 370 pp., MIT Press, Cambridge, MA, 1971.

Straub, G. K., J. M. Wills, and D. C. Wallace, Elastic moduli of copper under compressions, in *Shock Waves in Condensed Matter—1987*, edited by S. C. Schmidt and N. C. Holmes, Elsevier, New York, pp. 207–210, 1988.

Wang, G., An empirical expression of elastic sound speed of materials at high pressure, *Chin. J. High Pressure Phys.*, *2*, 92–95, 1988.

Wang, G., P. Xie, and Z. Tan, Radiometric measurements of overtaking rarefaction wave velocities in shock-loaded brass under high pressures, *Chin. J. High Pressure Phys.*, *1*, 144–149, 1987.